Dramatic Differences in the Binding of UDP-Galactose and UDP-Glucose to UDP-Galactose 4-Epimerase from *Escherichia coli*[†,‡]

James B. Thoden and Hazel M. Holden*

Department of Biochemistry, University of Wisconsin−Madison, 1710 University Avenue, Madison, Wisconsin 53705

Received April 20, 1998; Revised Manuscript Received May 28, 1998

ABSTRACT: UDP-galactose 4-epimerase catalyzes the interconversion of UDP-galactose and UDP-glucose during normal galactose metabolism. Within recent years the enzyme from *Escherichia coli* has been studied extensively by both biochemical and X-ray crystallographic techniques. One of several key features in the catalytic mechanism of the enzyme involves the putative rotation of a 4′-ketopyranose intermediate within the active site region. The mode of binding of UDP-glucose to epimerase is well understood on the basis of previous high-resolution X-ray crystallographic investigations from this laboratory with an enzyme/NADH/UDP-glucose abortive complex. Attempts to prepare an enzyme/NADH/UDP-galactose abortive complex always failed, however, in that UDP-glucose rather than UDP-galactose was observed binding in the active site. In an effort to prepare an abortive complex with UDP-galactose, a site-directed mutant protein was constructed in which Ser 124 and Tyr 149, known to play critical roles in catalysis, were substituted with alanine and phenylalanine residues, respectively. With this double mutant it was possible to crystallize and solve the three-dimensional structures of reduced epimerase in the presence of UDP-glucose or UDP-galactose to high resolution. This study represents the first direct observation of UDP-galactose binding to epimerase and lends strong structural support for a catalytic mechanism in which there is free rotation of a 4′-ketopyranose intermediate within the active site cleft of the enzyme.

UDP-galactose 4-epimerase, hereafter referred to as epimerase, catalyzes the interconversion of UDP-galactose and UDP-glucose and as such plays a critical role in galactose metabolism. As isolated from *Escherichia coli*, the enzyme is a homodimer with each subunit containing 338 amino acid residues and one tightly bound NAD^+ or NADH moiety (*1*−*3*). On the basis of high-resolution X-ray crystallographic studies, the enzyme from *E. coli* is known to fold into two distinct motifs as can be seen in Figure 1: an N-terminal or nucleotide-binding domain dominated by a seven-stranded parallel β-pleated sheet flanked on either side by α-helices and a smaller C-terminal domain responsible for the proper positioning of the UDP-sugar substrates (*3*−*5*). The active site cleft is wedged between these two domains.

According to all presently available biochemical and kinetic data, the reaction mechanism of epimerase is presumed to occur through a 4′-ketopyranose intermediate as shown in Scheme 1. Key features in this mechanism include the abstraction of the 4′-hydroxyl hydrogen of the sugar by an enzymatic base, the transfer of a hydride from C4 to NAD^+, and the rotation of the resulting 4′-ketopyranose intermediate in the active site to allow return of the hydride from NADH to the opposite face of the sugar. UDP-galactose 4-epimerase has attracted research attention due to several of its unique features including this nonstereospecificity of hydride return from the B-side of the nicotinamide ring of NADH to the 4′-ketopyranose intermediate and the putative rotation of this intermediate during the reaction mechanism.

In recent years, substantial structural progress has been made toward elucidating the identity of the catalytic base (*4*, *6*, *7*). From both X-ray crystallographic and site-directed mutagenesis studies it is now known that Ser 124, Tyr 149, and Lys 153, in concert, most likely function to abstract the 4′-hydroxyl hydrogen from the sugar substrate. Indeed, it has become apparent that the epimerase belongs to the superfamily of "short-chain" dehydrogenases which contain such a characteristic Tyr−Lys couple thought to function in catalysis (*5*, *8*, *9*). Other enzymes in this family, for which three-dimensional structures are available, include 3α,20β-hydroxysteroid dehydrogenase (*10*−*12*), dihydropteridine reductase (*13*, *14*), 7α-hydroxysteroid dehydrogenase (*15*), mouse lung carbonyl reductase (*16*), 17β-hydroxysteroid dehydrogenase (*17*, *18*), and dTDP-glucose 4,6-dehydratase (Thoden, unpublished results), among others.

With regard to the rotation of the 4′-ketopyranose intermediate in the active site, the structures of reduced epimerase complexed with UDP-glucose, UDP-mannose, UDP-4-deoxy-4-fluoro-α-D-galactose, or UDP-4-deoxy-4-fluoro-α-D-glucose have been determined and have shed light on the ability of the enzyme to accommodate different sugars (*4*, *19*). Obviously one of the critical candidates for additional structural studies is the epimerase/NADH/UDP-galactose abortive complex. Interestingly, all experiments designed to produce such a crystalline complex with native epimerase have been unsuccessful thus far (*4*). These attempts have included reduction of the enzyme with the dimethylamine/

[†] This research was supported in part by grants from the NIH (DK47814) and the NSF (BIR-9317398).

[‡] X-ray coordinates have been deposited in the Brookhaven Protein Data Bank (1A9Y and 1A9Z) and will be released upon publication.

* To whom correspondence should be addressed.

S0006-2960(98)00896-4 CCC: $15.00
Published on Web 07/29/1998

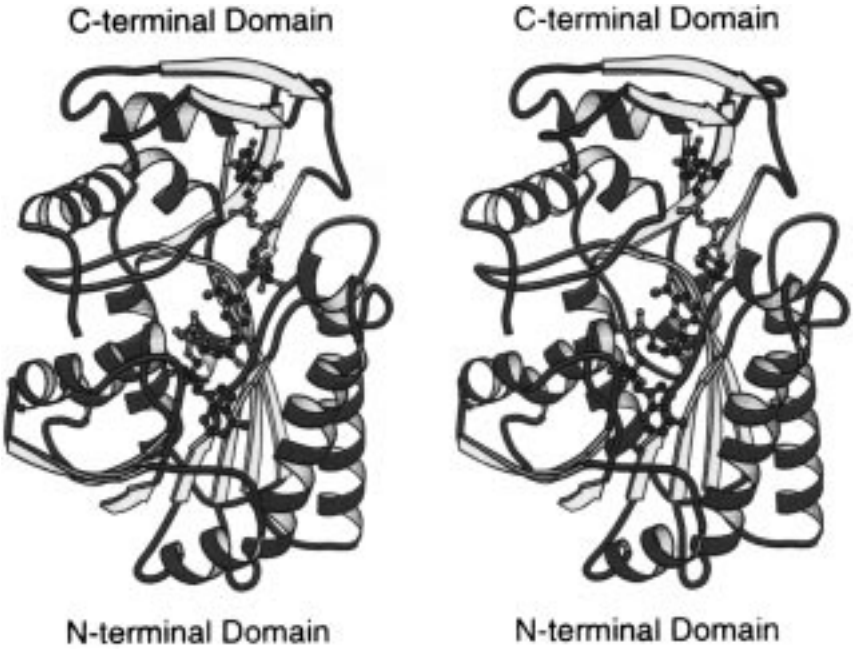

FIGURE 1: Ribbon representation of one subunit of UDP-galactose 4-epimerase from *E. coli*. This figure and Figures 3, 5, and 6 were prepared with the software package MOLSCRIPT (*29*). X-ray coordinates employed for this drawing were from Thoden et al. (*4*). The β-strands and α-helices are depicted in yellow and blue, respectively, while the NADH and UDP-glucose moieties are shown in ball-and-stick representations.

Scheme 1

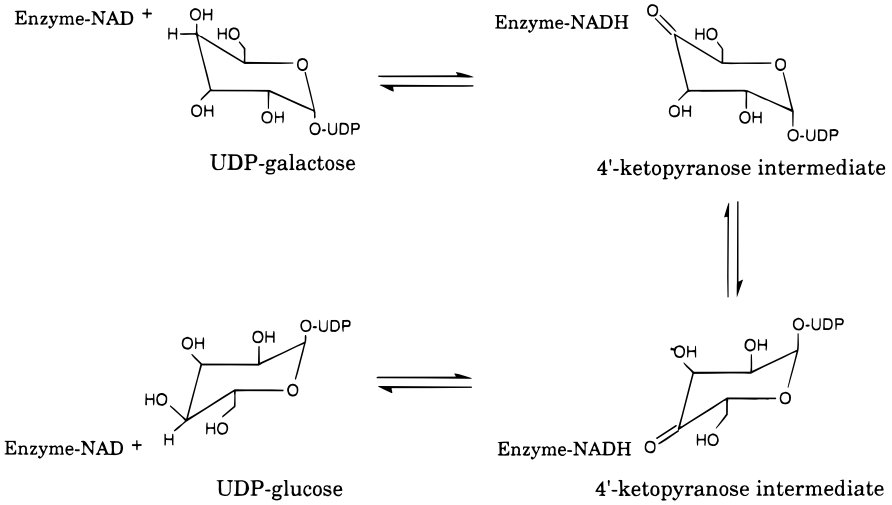

borane complex in the presence of UDP-galactose, UDP, UMP, or TMP and exchange of these nucleotides with UDP-galactose. In each case, the resulting electron density maps have clearly indicated the presence of UDP-glucose, rather than UDP-galactose, in the epimerase active site (*4*). Additionally, the same attempts with recombinant enzyme in which either Ser 124 or Tyr 149 had been changed to an alanine or phenylalanine residue, respectively, always resulted in UDP-glucose in the active site.

In attempt to explore the manner in which UDP-galactose binds in the epimerase active site, a double mutant of the protein, namely S124A·Y149F, was constructed, purified, and crystallized. Here we describe the successful attempt to prepare and solve the structure of a complex of epimerase with UDP-galactose. As a control, the three-dimensional structure of the S124A·Y149F protein with bound UDP-glucose was also determined to high resolution and described here. This investigation has allowed for a detailed comparison of the modes of binding of UDP-glucose and UDP-galactose in the epimerase active site and, indeed, provides structural support for a catalytic mechanism in which the sugar moiety freely rotates in the active site cleft.

MATERIALS AND METHODS

Construction of the Plasmid Containing the S124A·Y149F Mutations. The S124A·Y149F mutant plasmid was constructed starting with the Y149F mutant plasmid (*7*). The Y149F plasmid was digested with *Bss*HII and *Nde*I, the 5′-phosphate groups removed by treatment with calf intestinal phosphatase, and the resulting digested plasmid purified on a 1% agarose gel. A new mutagenic cassette was inserted into the resulting gap with the following complementary oligonucleotides: (1) S124A-top, CGCGCCCCAACGTCAAAAACTTTATTTTCTCGTCCGCGGCGGCCACCGTTTATGGCGATCAGCCCAAAATTCCA; (2) S124A-bottom, TATGGAATTTTGGGCTGATCGCCATAAACGGT-

Table 1: Intensity Statistics

	S124A·Y149F/NADH/UDP-Glucose Complex resolution range (Å)								
	overall	30.0−3.6	2.86	2.50	2.27	2.11	1.98	1.88	1.80
no. of measurements	84014	16461	20068	12161	9404	8188	7061	6140	4531
no. of independent reflections	37966	5366	5275	5067	4939	4761	4505	4347	3706
% completeness	91	98	100	98	94	94	83	83	74
av I/av $\sigma(I)$	15.0	29.9	17.6	9.4	5.8	4.2	3.0	2.3	1.9
R-factor[a] (%)	4.1	2.3	4.4	7.3	10.1	13.1	16.2	18.6	20.4
	S124A·Y149F/NADH/UDP-Galactose Complex resolution range (Å)								
	overall	30.0−3.8	3.02	2.63	2.39	2.22	2.09	1.99	1.90
no. of measurements	112562	22615	23568	18088	12824	11544	10094	8.117	5712
no. of independent reflections	32710	4566	4.374	4278	4187	4149	4017	3851	3288
% completeness	93	99	99	96	95	95	93	93	74
av I/av $\sigma(I)$	24.6	53.5	29.2	13.5	8.9	6.5	5.1	3.8	2.9
R-factor[a] (%)	4.6	2.8	4.1	8.2	10.6	13.2	16.3	19.9	22.8

[a] R-factor $= (\sum|I - \bar{I}|/\sum I) \times 100$.

Table 2: Least-Squares Refinement Statistics for the Epimerase/Sugar Complexes

	UDP-glucose	UDP-galactose
resolution limits (Å)	30.0−1.8	30.0−1.9
R-factor (%)[a]	18.2	18.9
no. of reflections used	37966	32710
no. of protein atoms	2704	2703
no. of solvent atoms	545[b]	554[c]
weighted RMSD from ideality		
bond length (Å)	0.012	0.008
bond angle (deg)	2.56	2.52
planarity (trigonal) (Å)	0.008	0.006
planarity (other planes) (Å)	0.012	0.013
average B-factors (Å^2)		
backbone atoms	20.6	27.0
all atoms	25.9	32.6

[a] R-factor $= \sum|F_o - F_c|/\sum|F_o|$, where F_o is the observed structure factor amplitude and F_c is the calculated structure factor amplitude. [b] These include 541 water molecules and 4 sodium ions. [c] These include 541 water molecules, 3 sodium ions, and 1 tri(ethylene glycol) molecule.

GGCCGCGGACGAGAAAATAAAGTTTTTGACGTTGGCGG. These oligonucleotides were obtained from Gibco BRL (Grand Island, NY). A silent *Sac*II restriction site was designed into the cassette to facilitate identification of the plasmid carrying the S124A mutation.

Purification and Crystallization Procedures. Recombinant UDP-galactose 4-epimerase was expressed in *E. coli* and purified according to previously published procedures (*3*). The standard assay for activity (*20*) revealed no measurable activity for this recombinant protein.

For crystallization trials, the recombinant enzyme, in 10 mM potassium phosphate (pH 7.0), was first incubated with the reducing agent, 50 mM dimethylamine/borane complex, for 1 h at room temperature. Subsequently, UDP-galactose (or UDP-glucose) was added to a concentration of 10 mM. The reaction was allowed to continue for 2 h, after which time additional reducing agent was added to a concentration of 150 mM. The reaction mixture was incubated overnight at 4 °C and then dialyzed against 10 mM potassium phosphate (pH 8.0) for 24 h at 4 °C. Following dialysis, the protein was concentrated to 35 mg/mL.

Large single crystals of both S124A·Y149F/NADH/UDP-sugar complexes were grown by the hanging drop method of vapor diffusion against 18−25% (w/v) poly(ethylene glycol) 8000, 400−800 mM NaCl, and 50 mM CHES (pH 9.0) at 4 °C. Crystals typically appeared within 6−12 h, and growth was generally complete within 4−5 days. The crystals, which were isomorphous to those previously described for the epimerase/NADH/UDP-glucose abortive complex (*4*), belonged to the trigonal space group $P3_221$ and contained one subunit per asymmetric unit. The unit cell dimensions for the S124A·Y149F/NADH/UDP-galactose complex and the S124A·Y149F/NADH/UDP-glucose complex were $a = b = 83.9$ Å, $c = 108.1$ Å and $a = b = 85.0$ Å, $c = 106.7$ Å, respectively.

X-ray Data Collection and Processing. Prior to X-ray data collection, the crystals were transferred to 25% (w/v) poly(ethylene glycol) 8000, 750 mM NaCl, 50 mM CHES (pH 9.0), 10 mM UDP-sugar, and 20% (v/v) ethylene glycol. Each crystal was suspended in a thin film of this cryoprotectant solution in a loop of fine surgical thread and flash-cooled in a nitrogen stream. All X-ray data were collected at −150 °C with a Siemens (Bruker) HI-STAR area detector system equipped with Goebel focusing optics. The X-ray source was Cu $K\alpha$ radiation from a Rigaku RU200 rotating anode generator operated at 50 kV and 90 mA and equipped with a 300 μm focal cup. Only one crystal was required per X-ray data set. These X-ray data were processed with the data reduction software package SAINT (Bruker AXS Inc.) and scaled with the program XCALIBRE (G. Wesenberg and I. Rayment, unpublished results). Relevant X-ray data collection statistics for the two crystalline complexes can be found in Table 1.

Structural Determination. The previously solved structure of the epimerase/NADH/UDP-glucose complex (*4*) served as the starting model for the least-squares refinements of the two S124A·Y149F/NADH/UDP-sugar complexes described here. The software package TNT (*21*) was employed for the refinements with ideal stereochemistries of the NADH, UDP, and sugar moieties based on the small molecule structural determinations of Reddy et al. (*22*), Viswamitra et al. (*23*), Glasfeld et al. (*24*), and Lonchambon et al. (*25*). Alternate cycles of manual model building with the program FRODO (*26*) and least-squares refinement reduced the R-factors to 18.9% (1.90 Å resolution) and 18.2% (1.8 Å

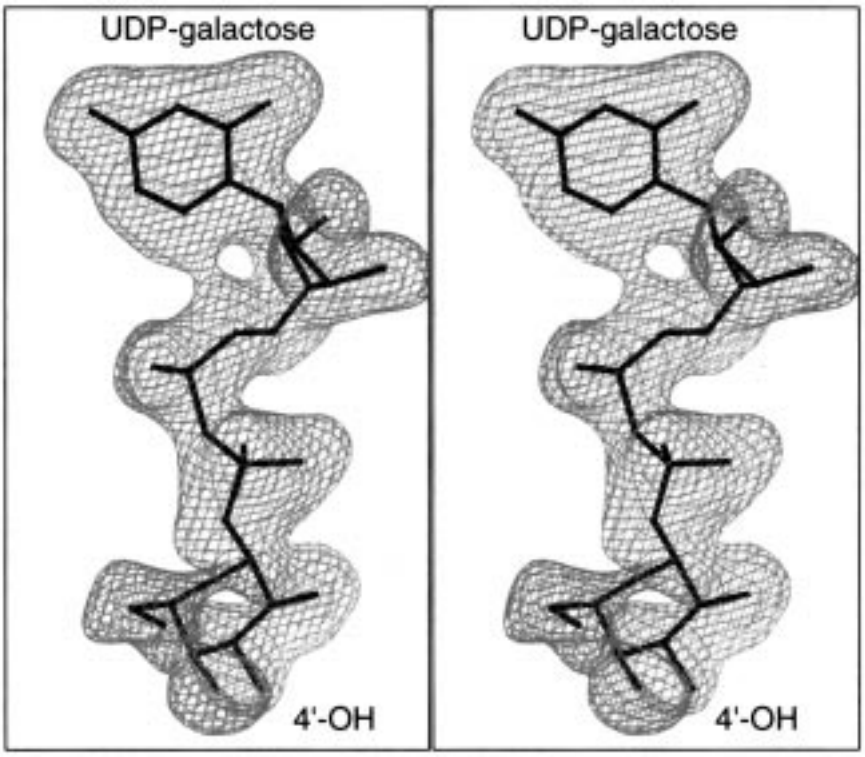

FIGURE 2: Electron density corresponding to the UDP-galactose ligand bound in the active site. The map shown was calculated with coefficients of the form ($F_o - F_c$), where F_o was the native structure factor amplitude and F_c was the calculated structure factor amplitude from the model lacking the coordinates for the UDP-galactose. The map was contoured at 2.5σ. This figure and Figure 4 were prepared with the software package FROST, written by Dr. Gary Wesenberg.

resolution) for the S124A·Y149F/NADH/UDP-galactose and S124A·Y149F/NADH/UDP-glucose complexes, respectively. Refinement statistics are given in Table 2. Ramachandran plots demonstrate that all non-glycinyl main chain dihedral angles lie within or near the allowed regions with the exception of Phe 178. In each complex, this residue adopts average ϕ,ψ angles of $-96.0°$ and $-118.0°$, respectively. Previous studies have shown that the side chain conformation of Phe 178, like that of Phe 218, is dependent upon the oxidation state of the dinucleotide cofactor (*3*). Also, in the S124A·Y149F/NADH/UDP-galactose and S124A·Y149F/NADH/UDP-glucose complexes, position 131 was modeled as an asparagine or glutamine, respectively. The electron density at position 131 was unambiguous for both complexes. This type of heterogeneity was previously observed in the structural analysis of the epimerase/NADH/UDP-mannose complex (*19*) and most likely reflects heterogeneity in the protein sample employed for the crystallization trials.

RESULTS

Description of the Y149F·S124A/NADH/UDP-Galactose Complex. The electron density corresponding to the UDP-galactose ligand is shown in Figure 2, and as can be seen, the sugar moiety is clearly that of galactose. The average *B*-factors for the UDP-galactose and NADH moieties are 30.5 and 21.9 Å^2, respectively. The polypeptide chain backbone of the Y149F·S124A/NADH/UDP-galactose complex is strikingly similar to that of the native epimerase such that the two proteins superimpose with a root-mean-square deviation (RMSD) of 0.13 Å for all backbone atoms.

A close-up view of the active site for this complex is shown in Figure 3a. As expected for a B-side specific enzyme, the nicotinamide ring of the reduced cofactor adopts the syn conformation, thereby presenting the proper *si* face for hydride transfer from C4 of the UDP-galactose to C4 of the dinucleotide cofactor. The observed distance between C4 of the galactose and C4 of the nicotinamide ring is 3.5 Å. In the native epimerase/NADH/UDP-glucose model, this distance is comparable at 3.7 Å. On the basis of both X-ray crystallographic and site-directed mutagenesis studies, it has been postulated that Ser 124 and Tyr 149 play critical roles in catalysis (*4*−*7*). While these positions have been changed to an alanine and phenylalanine, respectively, for the investigation described here, they still adopt exceedingly similar positions within the epimerase active site. Specifically, in the Y149F·S124A/NADH/UDP-galactose complex, the 4′-hydroxyl group of the sugar moiety is located at 3.3 and 5.1 Å, respectively, from C^β of Ala 124 and C^ζ of Phe 149. These distances in the native epimerase/NADH/UDP-glucose are 3.8 and 4.4 Å (*4*).

Potential hydrogen-bonding interactions between the protein and the sugar substrate are indicated by the dashed lines in Figure 3b. There are 16 electrostatic interactions within 3.0 Å between the enzyme and the UDP-galactose ligand and 5 well-ordered water molecules surrounding the substrate. The uracil ring is anchored to the protein via the backbone carbonyl and amide groups of Ala 216 and Phe 218, respectively, while the 2′-hydroxyl group of the ribose interacts with the carboxylate side chain of Asp 295. Those amino acids responsible for hydrogen bonding to the phosphate groups of the ligand include Asn 179, Arg 231, and Arg 292. The 2′-hydroxyl group of the galactose is hydrogen bonded to Tyr 299 and Asn 179 while the 3′-hydroxyl group lies within 3.0 Å of the carbonyl groups

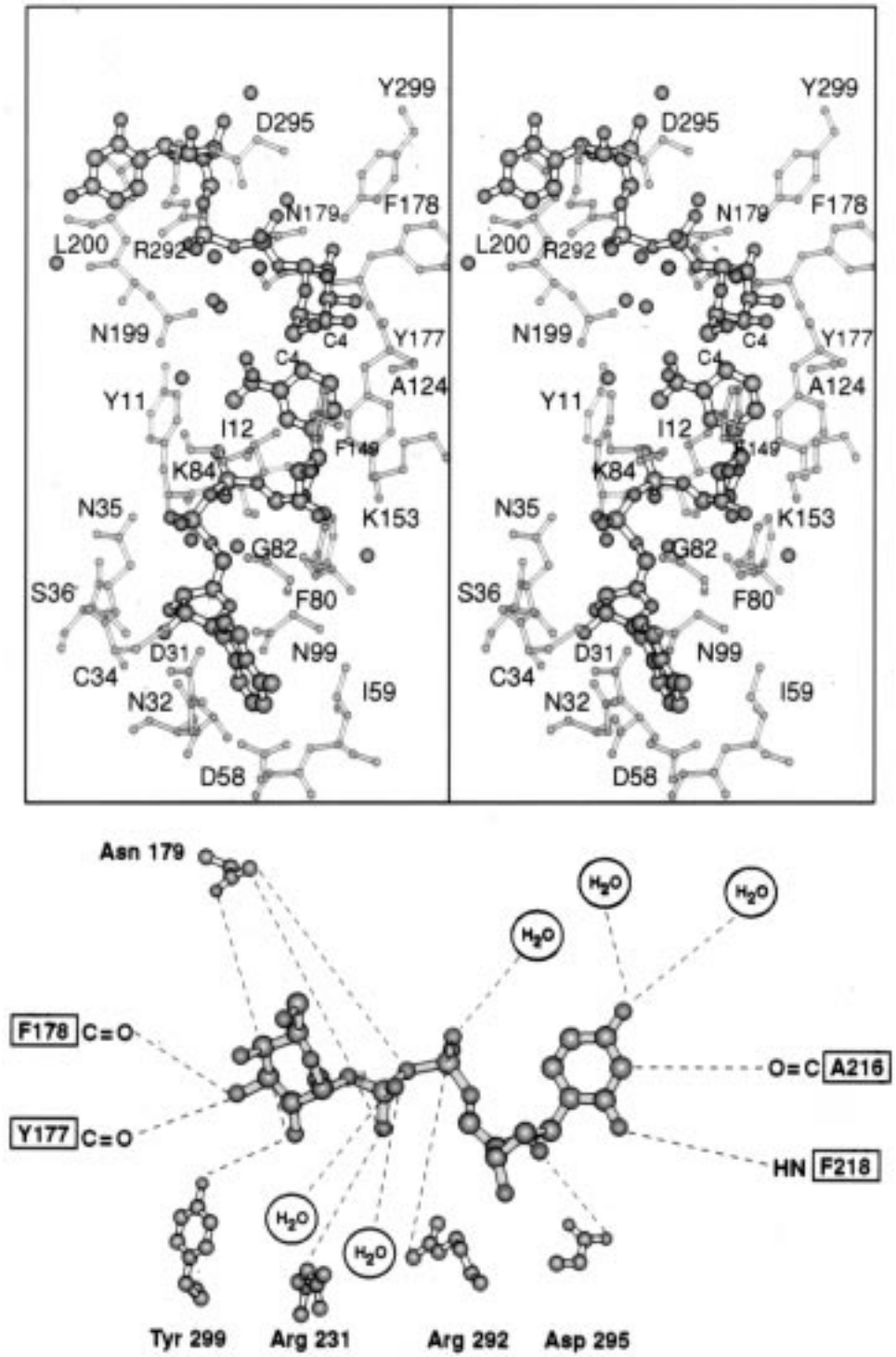

FIGURE 3: Close-up view of the active site for the S124A·Y149F/NADH/UDP-galactose complex. Shown in (a) are those amino acid residues located within approximately 3.2 Å of atoms of the NADH and UDP-galactose molecules. For the sake of clarity near the UDP molecule, Ala 216, Phe 218, and Arg 231 were omitted from this drawing. The interactions between the UDP-galactose molecule and these residues are indicated in the cartoon drawing given in (b). Potential hydrogen bonds, within 3.0 Å, between the UDP-galactose molecule and the protein are indicated by the dashed lines.

of Tyr 177 and Phe 178. Note that the 4′-hydroxyl group does not interact with the protein within 3.0 Å. In the native epimerase/NADH/UDP-glucose model this hydroxyl group is located at 2.6 Å from O^{γ} of Ser 124 (*4*).

Description of the Y149F·S124A/NADH/UDP-Glucose Complex. In an effort to ensure that the observed binding of UDP-galactose to the Y149F·S124A protein was not an artifact resulting from the employment of a site-directed mutant, the structure of the Y149F·S124A/NADH/UDP-glucose complex was also determined and compared to that previously determined for the native epimerase abortive complex (*4*). Electron density corresponding to the UDP-glucose ligand is displayed in Figure 4. The average *B*-values for the UDP-glucose and NADH moieties are 20.5 and 16.1 $Å^2$, respectively. The polypeptide chain backbone atoms for the Y149F·S124A/NADH/UDP-glucose complex and the epimerase/NADH/UDP-glucose abortive complex (*4*) superimpose with a RMSD of 0.16 Å for all backbone atoms.

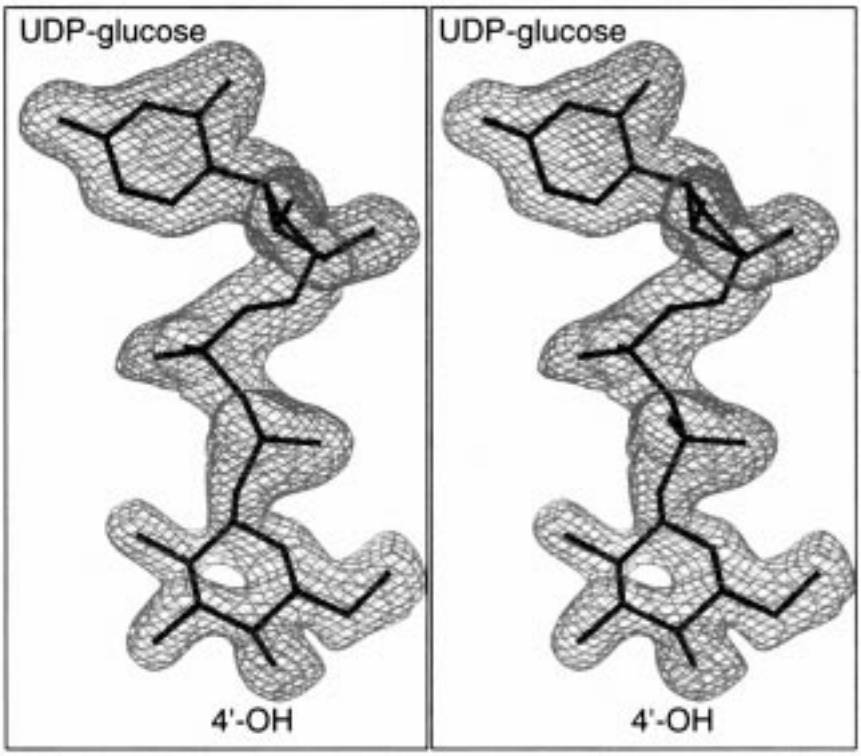

FIGURE 4: Electron density corresponding to the UDP-glucose ligand bound in the active site. The map shown was calculated according to the method described in Figure 2 and was contoured at 4σ.

Clearly, the replacement of the amino acids at positions 124 and 149 resulted in little perturbation of the overall molecular architecture of the enzyme. As a further indication of the three-dimensional similarities between the two models, the UDP-glucose and NADH moieties superimpose with a RMSD of 0.19 Å.

A close-up view of the active site for the Y149F•S124A/NADH/UDP-glucose complex is shown in Figure 5. Again, the nicotinamide ring presents the *si* face to the glucose moiety with C4 of the cofactor lying within 3.9 Å of C4 of the glucose. The 4′-hydroxyl group of the glucose moiety is positioned at 3.5 Å from C^{β} of Ala 124 and 5.0 Å from C^{ζ} of Phe 149. There are 10 well-ordered water molecules surrounding the UDP-glucose as indicated in Figure 5b and 22 potential hydrogen bonds within 3.0 Å between the protein, the substrate, and the solvent. As described above for the Y149F•S124A/NADH/UDP-galactose complex, the uracil ring forms hydrogen bonds with the backbone carbonyl and amide groups of Ala 216 and Phe 218, respectively, and the carboxylate group of Asp 295 serves to anchor the 2′-hydroxyl group of the ribose to the protein. In addition to Asn 179, Arg 231, and Arg 292, the carboxamide group of Asn 199 and the backbone amide group of Leu 200 also participate in hydrogen-bonding interactions with the phosphoryl oxygens due to a translation, relative to that observed for UDP-galactose, of these atoms within the active site. As observed in the binding of UDP-galactose, both Tyr 299 and Asn 179 interact with the hexose portion of the substrate. In this case, however, both O^{η} of Tyr 299 and $O^{\delta 1}$ of Asn 179 hydrogen bond to the 6′-hydroxyl, rather than the 2′-hydroxyl group. Clearly, the side chain groups of Asn 179 and Tyr 299 provide, in combination, a proper template for productive substrate binding of either UDP-glucose or UDP-galactose.

DISCUSSION

One of the unique features characterizing the epimerase reaction mechanism is the putative rotation of the 4′-ketopyranose within the active site. Over 20 years ago, the nonstereospecificity displayed by epimerase was suggested to occur through a simple rotation of the intermediate about the bond connecting the glycosyl oxygen atom and the β-phosphorus atom in the pyrophosphoryl linkage (*27*). The results from this study have shown that, indeed, there is such a rotation, albeit not as simple as once envisioned. Shown in Figure 6 is the superposition of the Y149F•S124A/NADH/UDP-galactose and Y149F•S124A/NADH/UDP-glucose complexes near the sugar residues. Although not shown in Figure 6, it should be noted that the uridine portions of the two substrates superimpose with a RMSD of 0.13 Å. As can be seen in Figure 6, significant structural changes between the two bound substrates begin to occur at the β-phosphorus atoms where their positions differ relative to one another by 0.51 Å. Due to this translation, the corresponding glycosyl oxygens differ by 1.2 Å. Significant changes also occur in two of the dihedral angles defining the substrate conformation, namely, those delineated by the α,β-bridging oxygen, the β-phosphorus, the glycosyl oxygen, and the hexose C1 and those delineated by the β-phosphorus, the glycosyl oxygen, and the hexose C1 and C2. These differences in torsional angles allow for the C4 position of the sugar to be oriented appropriately for B-side specific hydride transfer to the nicotinamide ring of the NAD^+. In the UDP-glucose and UDP-galactose substrates discussed here, these two dihedral angles differ by approximately 130° and 30°, respectively. Both changes in these two dihedral angles and translations of the pyrophosphoryl backbones also allow for the 4′-hydroxyl groups of the glucose and galactose substrates

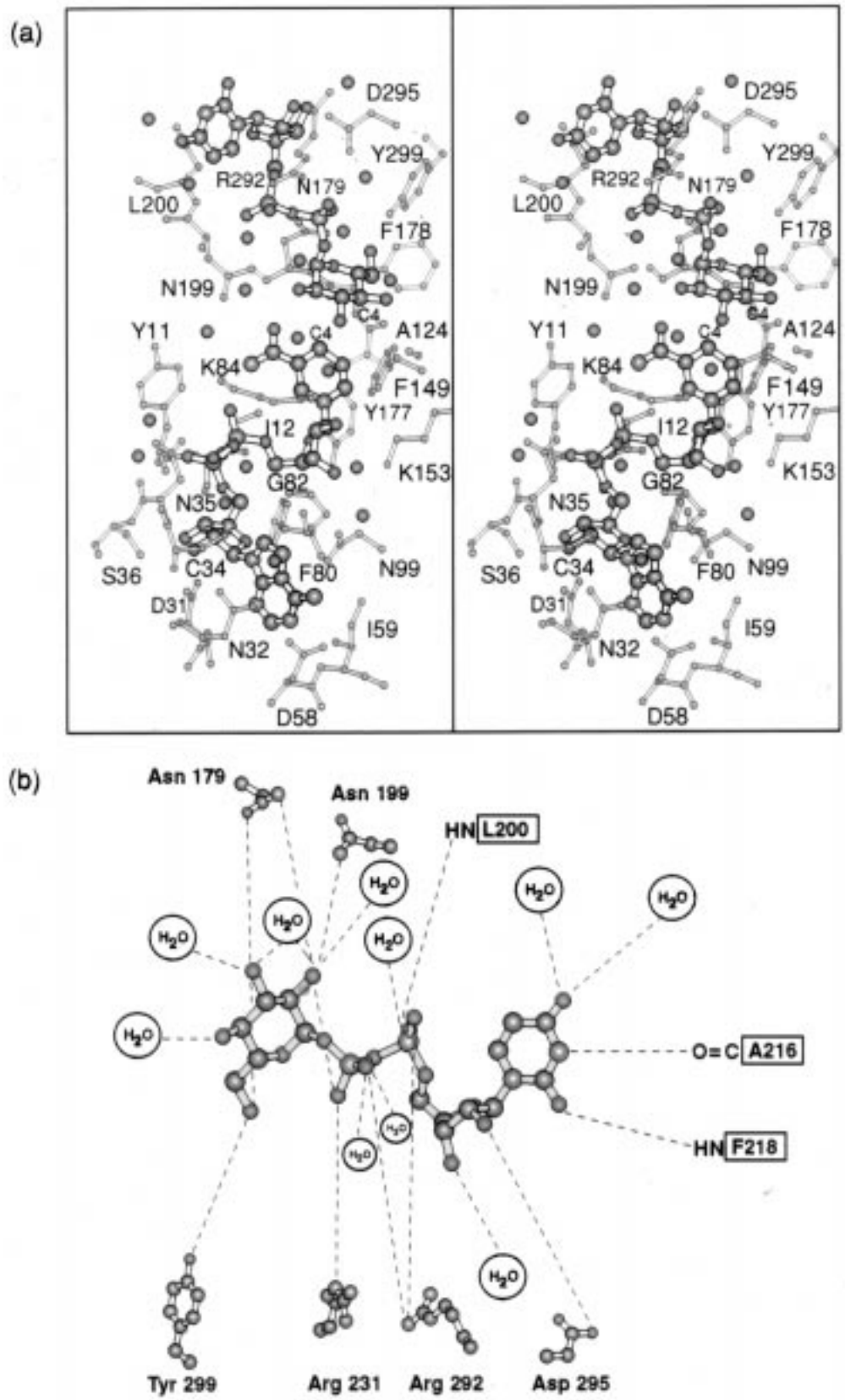

FIGURE 5: Close-up view of the active site for the S124A·Y149F/NADH/UDP-glucose complex. Shown in (a) are those amino acid residues located within approximately 3.2 Å of atoms of the NADH and UDP-glucose molecules. A cartoon depicting the potential hydrogen-bonding interactions between the UDP-glucose molecule and the protein, within 3.0 Å, is given in (b). Hydrogen bonds are indicated by the dashed lines. As in Figure 3, Ala 216, Phe 218, and Arg 231 were omitted from (a) for the sake of clarity.

to interact with Ala 124 (Ser in the native enzyme) and Phe 149 (Tyr in the native enzyme) in analogous manners. Other than the changes shown in Figure 6, the structures of the two protein complexes are virtually identical with all atoms, including side chains, superimposing with a RMSD of 0.41 Å. The active site of the enzyme is clearly large enough to

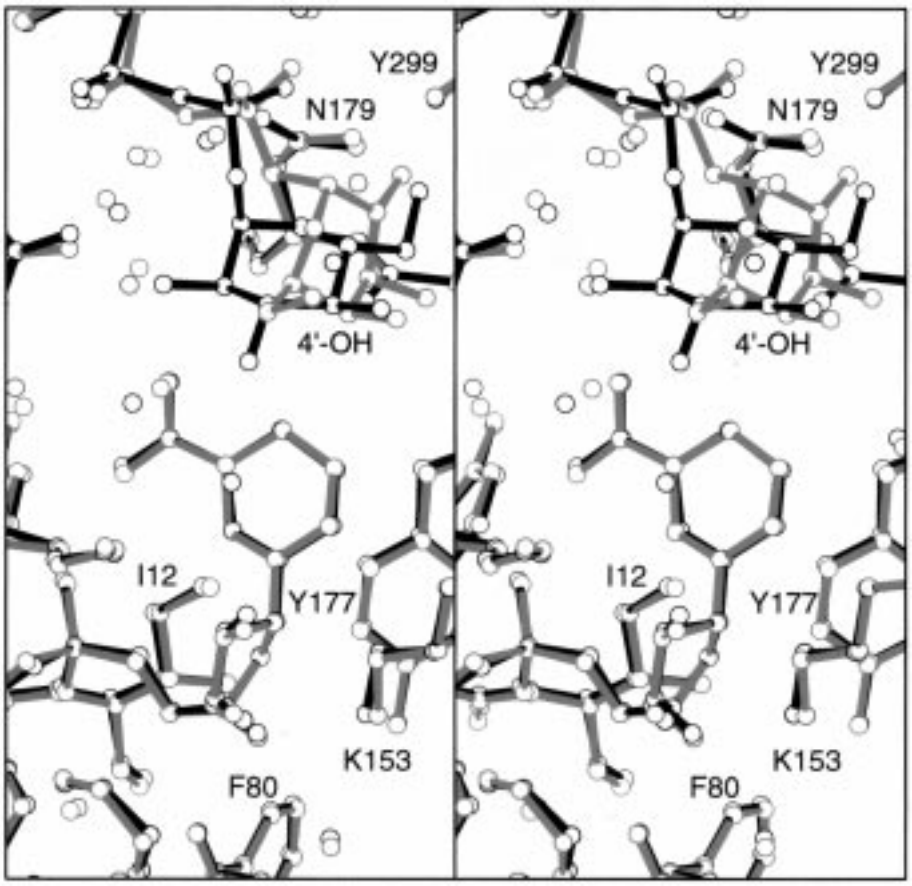

FIGURE 6: Superposition of the active sites for the S124A·Y149F/NADH/UDP-galactose and S124A·Y149F/NADH/UDP-glucose complexes. The S124A·Y149F/NADH/UDP-galactose and S124A·Y149F/NADH/UDP-glucose complexes are displayed in red and black, respectively.

easily accommodate the two sugar substrates without any concomitant movements in either polypeptide chain backbone or side chain atoms.

Although it was possible to successfully solve the structure of the epimerase/NADH/UDP-glucose abortive complex several years ago, until this present study, all efforts to prepare an epimerase/NADH/UDP-galactose abortive complex failed. From the investigation described here it is apparent that the greater number of interactions within 3.0 Å between the UDP-glucose substrate and epimerase versus the UDP-galactose ligand and the enzyme may have been a contributing factor to such failure. Any residual activity left in the enzyme, even after reduction with dimethylamine/borane, resulted in the conversion of the UDP-galactose to UDP-glucose, which is more tightly bound to the reduced enzyme. By employing the Y149F·S124A mutant protein as described here, it was possible to slow the conversion of UDP-galactose to UDP-glucose enough to allow for its investigation by X-ray crystallographic techniques.

In summary, this structural analysis has allowed for the first direct visualization of UDP-galactose binding within the active site of epimerase. Until now, the presumed manner in which this substrate bound to the enzyme was based solely on model-building studies. In addition, this research has revealed that Asn 179 and Tyr 299 form a template that allows for the proper positioning of the appropriate sugar residue within the active site. In the case of UDP-galactose, these side chain functional groups interact with the 2′-hydroxyl group, while for UDP-glucose, they form hydrogen bonds with the 6′-hydroxyl group of the sugar. Taken together, the two X-ray crystallographic models presented here, indeed, strongly support a catalytic mechanism requiring the rotation of an intermediate within the active site.

There are two very important structural issues concerning this fascinating enzyme that still need to be addressed, however. One of these concerns the conformational changes that occur when the enzyme binds the UDP-sugar substrate. According to present theories, substrate binding to epimerase leads to a conformational change in the enzyme which has the effect of activating the cofactor toward reduction (*27*, *28*). To date, all known three-dimensional structures of epimerase have either UDP, UDP-sugar, or UDP-phenol bound within the active site (*3*−*7*, *19*). To more fully understand those conformational changes that occur upon substrate binding, it will be necessary to solve the structure of the resting enzyme in which the UDP-sugar binding site is unoccupied. This work is in progress. The second issue concerns the catalytic mechanism which presumably involves both Ser 124 and Tyr 149. The working model at the present time implicates Ser 124, which is located at 2.6 Å from the 4′-hydroxyl group of glucose, and presumably galactose as well, as a proton shuttle between the sugar and the phenolic side chain of Tyr 149. Accordingly, Tyr 149, rather than Ser 124, is the ultimate catalytic base (*5*). The distance between O^{η} of Tyr 149 and O^{γ} of Ser 124 is 4.6 Å in the epimerase/NADH/UDP-glucose model, however, which is longer than would be expected for an efficient proton

network. The one caveat with all of the structural studies accomplished thus far, however, is that the observed distances between the side chain hydroxyls of Ser 124 and Tyr 149 are based on abortive, dead-end complexes. One obvious question concerns the positions of the these side chains in a productive epimerase/NAD^+/UDP-glucose or -galactose complex. In such a complex, are the side chains of Ser 124 and Tyr 149 closer than 4.6 Å as would be expected for such a proton network? If not, then what other factors are involved in the catalytic mechanism? Attempts to prepare such types of complexes with NAD^+ rather than NADH and with various site-directed mutant proteins are in progress as well.

ACKNOWLEDGMENT

We thank Dr. W. W. Cleland for critically reading the manuscript and for his suggestion of employing the S124A·Y149F site-directed mutant protein for these studies.

REFERENCES

1. Wilson, D. B., and Hogness, D. S. (1969) *J. Biol. Chem. 244*, 2132−2136.
2. Lemaire, H. G., and Müller-Hill, B. (1986) *Nucleic Acids Res. 14*, 7705−7711.
3. Thoden, J. B., Frey, P. A., and Holden, H. M. (1996) *Biochemistry 35*, 2557−2566.
4. Thoden, J. B., Frey, P. A., and Holden, H. M. (1996) *Biochemistry 35*, 5137−5144.
5. Thoden, J. B., Frey, P. A., and Holden, H. M. (1996) *Protein Sci. 5*, 2149−2161.
6. Thoden, J. B., Gulick, A. M., and Holden, H. M. (1997) *Biochemistry 36*, 10685−10695.
7. Liu, Y., Thoden, J. B., Kim, J., Berger, E., Gulick, A. M., Ruzicka, F. J., Holden, H. M., and Frey, P. A. (1997) *Biochemistry 36*, 10675−10684.
8. Baker, M. E., and Blasco, R. (1992) *FEBS Lett. 301*, 89−93.
9. Holm, L., Sander, C., and Murzin, A. (1994) *Nat. Struct. Biol. 1*, 146−147.
10. Ghosh, D., Weeks, C. M., Grochulski, P., Duax, W. L., Erman, M., Rimsay, R. L., and Orr, J. C. (1991) *Proc. Natl. Acad. Sci. U.S.A. 88*, 10064−10068.
11. Ghosh, D., Wawrzak, Z., Weeks, C. M., Duax, W. L., and Erman, M. (1994) *Structure 2*, 629−640.
12. Ghosh, D., Erman, M., Wawrzak, Z., Duax, W. L., and Pangborn, W. (1994) *Structure 2*, 973−980.
13. Varughese, K. I., Skinner, M. M., Whiteley, J. M., Matthews, D. A., and Xuong, N. H. (1992) *Proc. Natl. Acad. Sci. U.S.A. 89*, 6080−6084.
14. Varughese, K. I., Xuong, N. H., Kiefer, P. M., Matthews, D. A., and Whiteley, J. M. (1994) *Proc. Natl. Acad. Sci. U.S.A. 91*, 5582−5586.
15. Tanaka, N., Nonaka, T., Tanabe, T., Yoshimoto, T., Tsuru, D., and Mitsui, Y. (1996) *Biochemistry 35*, 7715−7730.
16. Tanaka, N., Nonaka, T., Nakanishi, M., Deyashiki, Y., Hara, A., and Mitsui, Y. (1996) *Structure 4*, 33−45.
17. Ghosh, D., Pletnev, V. Z., Zhu, D.-W., Wawrzak, Z., Duax, W. L., Pangborn, W., Labrie, F., and Lin, S.-X. (1995) *Structure 3*, 503−513.
18. Azzi, A., Rehse, P. H., Zhu, D.-W., Campbell, R. L., Labrie, F., and Lin, S.-X. (1996) *Nat. Struct. Biol. 3*, 665−668.
19. Thoden, J. B., Hegeman, A. D., Wesenberg, G., Frey, P. A., and Holden, H. M. (1997) *Biochemistry 36*, 6294−6304.
20. Wilson, D. B., and Hogness, D. S. (1964) *J. Biol. Chem. 239*, 2469−2481.
21. Tronrud, D. E., Ten Eyck, L. F., and Matthews, B. W. (1987) *Acta Crystallogr. A43*, 489−501.
22. Reddy, B. S., Saenger, W., Mühlegger, K., and Weimann, G. (1981) *J. Am. Chem. Soc. 103*, 907−914.
23. Viswamitra, M. A., Post, M. L., and Kennard, O. (1979) *Acta Crystallogr. B35*, 1089−1094.
24. Glasfeld, A., Zbinden, P., Dobler, M., Benner, S. A., and Dunitz, J. D. (1988) *J. Am. Chem. Soc. 110*, 5152−5157.
25. Lonchambon, F., Avenel, D., and Neuman, A. (1976) *Acta Crystallogr. B32*, 1882.
26. Jones, T. A. (1985) *Methods Enzymol. 115*, 157−171.
27. Kang, U. G., Nolan, L. D., and Frey, P. A. (1975) *J. Biol. Chem. 250*, 7099−7105.
28. Bertland, A. U., and Kalckar, H. M. (1968) *Proc. Natl. Acad. Sci. U.S.A. 61*, 629−635.
29. Kraulis, P. J. (1991) *J. Appl. Crystallogr. 24*, 946−950.

BI9808969